

Anionic lipids modulate little the reorganization effect of amyloid-beta peptides on membranes

Oleksandr Ivankov¹, Dina R. Badreeva², Elena V. Ermakova¹, Tomáš Kondela³,
Tatiana N. Murugova¹ and Norbert Kučerka^{1,4}

¹ Frank Laboratory of Neutron Physics, Joint Institute for Nuclear Research, Dubna, Russia

² Meshcheryakov Laboratory of Information Technologies, Joint Institute for Nuclear Research, Dubna, Russia

³ Department of Nuclear Physics and Biophysics, Faculty of Mathematics, Physics and Informatics, Comenius University Bratislava, Bratislava, Slovakia

⁴ Department of Physical Chemistry of Drugs, Faculty of Pharmacy, Comenius University Bratislava, Bratislava, Slovakia

Abstract. Amyloid- β peptide interactions with model lipid membranes have been studied by means of small angle neutron scattering and molecular dynamics simulations. These interactions had been indicated recently as an origin of the membrane structure reorganizations between spherical small unilamellar vesicles and planar bicelle-like structures. In present work, we investigate the influence of charge on the peptide-triggered morphological changes by introducing the anionic lipid DMPS to the underlying DMPC membrane. Changes to the membrane thickness and the overall membrane structure with and without A β_{25-35} incorporated have been investigated over a wide range of temperatures. Our results document the previously reported morphological reformations between bicelle-like structures present in gel phase and small unilamellar vesicles present in fluid phase to be independent from the charge existence in the system.

Key words: Amyloid- β peptide — Anionic phosphatidylcholine membrane — Lipid phase transition — Peptide-lipid interactions — Small angle neutron scattering — Molecular dynamics

Abbreviations: A β , amyloid- β peptide; BLS, bicelle-like structure; DMPC, 1,2-dimyristoyl-sn-glycero-3-phosphocholine; DMPS, 1,2-dimyristoyl-sn-glycero-3-phospho-L-serine (sodium salt); DSC, differential scanning calorimetry; EULV, extruded unilamellar vesicle; MD, molecular dynamics; SANS, small angle neutron scattering; SULV, small unilamellar vesicle; TFA, 2,2,2-trifluoroacetic acid; TFE, 2,2,2-trifluoroethanol; ULV, unilamellar vesicle.

Introduction

One of the key factors of Alzheimer's disease is considered to be the amyloid- β peptide (A β) and its self-aggregation into large fibrils (Wildburger et al. 2017; Selivanova et al. 2018).

It is a peptide cleaved from amyloid precursor protein *via* enzymatic processes that originate in the cell membrane. The ability of A β itself to interact with the membrane was found to depend on the structural and elasto-mechanical properties of the membrane, thus its thermodynamic phase

Correspondence to: Oleksandr Ivankov, Frank Laboratory of Neutron Physics, Joint Institute for Nuclear Research, Dubna, Russia
E-mail: ivankov@jinr.ru

Norbert Kučerka, Department of Physical Chemistry of Drugs, Faculty of Pharmacy, Comenius University Bratislava, Bratislava, Slovakia
E-mail: kucerka@nf.jinr.ru

© The Authors 2023. This is an **open access** article under the terms of the Creative Commons Attribution-NonCommercial 4.0 International License (<https://creativecommons.org/licenses/by-nc/4.0/>), which permits non-commercial use, distribution, and reproduction in any medium, provided the original work is properly cited.

(Yoda et al. 2008; Buchsteiner et al. 2010). In fact, our previous findings show an intriguing temperature-dependent morphological reorganization of model membrane systems containing A β _{25–35} – the reorganization that was concluded as a result of temporal destruction of the membrane during its phase transition (Ivankov et al. 2021). The model membrane in that study consisted solely of the zwitterionic phosphatidylcholines. However, recent studies show the strong interactions also between A β peptide and negatively charged lipids (Dante et al. 2002; Bokvist et al. 2004; Buchsteiner et al. 2010, 2012; Sugiura et al. 2015; Heo et al. 2021). It then becomes interesting to investigate the influence of the charge on the previously reported peptide-triggered morphological reorganization in the model lipid system.

Hellstrand et al. (2010) show, that there is almost no difference between the fibril formations in the presence of neutral or negatively charged lipid systems. Another behavior is, however, documented in the investigations of the fibrillation process when the A β was incubated with lipid vesicles (Heo et al. 2021). We note that the peptide starts to aggregate at concentrations above 10% (Tang et al. 2016). In addition, the fibrillation process exhibits a strong dependence on the lipid packing density as well as the charge of the membrane. Apparently, the charge supports the fibril formation in the systems with the A β added to the EULVs externally (spherical object, bound by a single bilayer of lipids, containing aqueous solution inside, with its size predetermined by the extrusion through the pores of given size). At the same time, however, the findings of Bokvist et al. (2004) show, that anionic lipids could prevent the peptide releasing from the membrane after it was incorporated therein. One could conclude that the peptide incorporated into such membrane cannot move out into the outside environment, and the peptide present outside the membrane cannot cross to its interior. These results then underline the role of the peptide initial incorporation into the membrane.

The difference caused by the presence of charged lipids has been shown also in the case of the location of A β in lipid bilayers. The results of neutron diffraction analysis by the authors in (Dante et al. 2002; Dies et al. 2014) show that A β is located primarily in the hydrophobic region in the case of neutral membrane, while in the charged systems it is found to be almost equally distributed between the membrane hydrophilic (lipid headgroups) and hydrophobic (lipid tails) regions. This is true for both the short (25–35) and full fragment (1–42) A β . In addition, the studies show the two fragments cause little difference regarding their influence on the membrane fluidity (Buchsteiner et al. 2010) and other mechanical properties, as well as their toxicity (Kubo et al. 2002; Accardo et al. 2014).

Further, the incorporation of A β disturbs the membrane by accelerating the lateral diffusion therein, as has been shown for the DMPC/DMPS membranes in their liquid

crystalline phase (Buchsteiner et al. 2012). This is apparently a common property of A β , while other peptides most often tend to decrease the lateral diffusion (Pampel et al. 2003; Orädd and Lindblom 2004). The short A β _{25–35} in particular increases the lipid mobility and increases the short-range flexibility of the membrane (Buchsteiner et al. 2010) which could relate to the A β propensity for interactions with the highly curved SULVs (Sugiura et al. 2015). In the latter, A β tends to adopt α -helical conformation in the gel phase membranes (Sugiura et al. 2015), while it transitions to β -sheet structures with the increasing density of peptide on the surface of liquid-crystalline membranes. One can imagine these transitions being the underlying mechanism of membrane reformations between highly curved SULVs in the liquid-crystalline phase and flattened BLS (disk-shaped object formed by the single lipid bilayer and possibly with A β on their edges (Ivankov et al. 2021)). Consequently, the temporal destruction of the membrane would relate to the changes of elasto-mechanical properties of the membrane, rather than the presence of charged lipids in the membrane.

Materials and Methods

Sample preparation

DMPC and DMPS from Avanti Polar Lipids (Alabaster, AL) and A β segment 25–35 (A β _{25–35}) from Abbiotec (Escondido, CA) were purchased in lyophilized powder form and used without further purification. Organic solvents TFE and chloroform, and TFA were purchased from Sigma Aldrich.

Lipids were dissolved separately in an organic solvents mixture of chloroform:TFE = 1:1 (by volume) in glass vials at the total concentration of 50 mg/ml for DMPC and 2 mg/ml for DMPS. The peptide was subjected to a pretreatment procedure, according to which it was dissolved in TFA and treated in ultrasonic bath for 10–12 min for ensuring a peptide disaggregation (Barrett et al. 2015). Acid solution was then evaporated under a stream of nitrogen and the peptide was redissolved in the same organic solvent as lipids at a concentration of 2 mg/ml.

Required amount of each lipid solution was mixed in microtubes to reach the DMPS concentration 0.5, 1, 2 and 3% (mol/mol) comparable to the concentrations in previously published studies (Dante et al. 2002). Then, 3% A β _{25–35} (mol/mol) was added to the lipid mixture. Such concentration was selected to diminish the possibility of its spontaneous aggregation and bilayer structure disruption (Dies et al. 2014). The samples were dried to dryness and placed under vacuum for 12 h for removing the remaining solvent. The lipid and lipid/A β _{25–35} films were then hydrated with D₂O at the total concentration of 1% (by mass). The hydrated samples were frozen and thawed in several cycles

accompanied with a thorough vortexing. The attention was paid to keeping the samples at temperatures below the lipid phase transition to its fluid phase at all times (temperatures below 22°C).

The resulting multilamellar solutions were finally extruded into EULV. The Avanti Mini Extruder[®] was utilized in a room kept at the given temperature without additional heating. It was fitted with polycarbonate membranes of pore sizes 500 Å.

Differential scanning calorimetry

DSC measurements were performed on Nano DSC differential scanning calorimeter (TA Instruments, USA) at Faculty of Pharmacy, Comenius University Bratislava (Bratislava, Slovakia). Similar procedure for sample preparation was used as mentioned above, while redistilled H₂O water was used instead of D₂O and final concentration was diluted to 5 mg/ml. Prior to measurements, samples and the reference buffer (redistilled water) were degassed for at least 15 min. All samples were scanned eight to nine times for the reproducibility confirmation. Scans were carried out over the ranges from 5 to 50°C using a scanning rate of 1°C/min. Normalization to mass curves were calculated using NanoAnalyze Software.

Small angle neutron scattering experiments

SANS measurements were performed at the time-of-flight spectrometer YuMO at the IBR-2 pulsed reactor (JINR, Dubna, Russia) in two-detector mode (Kuklin et al. 2017). The two circular wire-ring detectors were placed at distances 4.5 and 13 m from the sample, which allowed covering the q-range from 0.007 to 0.3 Å⁻¹. The neutron beam was formed by a set of two pinhole collimators of diameters 40 and 14 mm. The vanadium standard was used for absolute intensity calibration. Raw data treatment was performed in the SAS program (Soloviev et al. 2017). The samples were contained in 1-mm-thick flat quartz cuvettes (Hellma) and held in the multipositional sample holder connected to the Lauda liquid thermostat with a temperature accuracy of $\pm 0.03^\circ\text{C}$. The collected scattering curves were corrected for background scattering from the buffer solution. The analysis of final SANS curves including the error analysis was performed with the SASFit program (Breßler et al. 2015) using the models of bilayered vesicles or randomly oriented cylindrical core-shell objects with a circular cross-section (Ivankov et al. 2021).

Molecular dynamics simulations

The behavior of A β_{25-35} peptide in a model phospholipid membrane and its effect on membrane properties was investigated also utilizing a set of MD simulations. The simulations were performed using the GROMACS 2019.3 software pack-

age (Van Der Spoel et al. 2005) and the all-atom CHARMM36 force field (Klauda et al. 2010). The initial configurations and topologies of the model bilayers containing 256 DMPC/DMPS molecules, 8 A β_{25-35} molecules, and 50 water molecules *per lipid* were set up using Membrane Builder from the CHARMM-GUI (Jo et al. 2008). The bonds with H-atoms were constrained using the LINKS algorithm, force-based switching functions with a range of 1.0–1.2 nm were used for the Lennard-Jones interactions, and long-range electrostatic interactions were calculated using the particle mesh Ewald algorithm. Periodic boundary conditions were used in all three dimensions. The integration of the motion equations was performed using the leapfrog algorithm with a time step of 2 fs. The systems were coupled to the Berendsen thermostat at 293 K, 303 K, and 323 K with a coupling time constant of 1 ps, while the pressure was maintained at 1 bar using a semi-isotropic pressure coupling with the Berendsen barostat. For production runs, the thermostat and barostat were switched to those of Nose-Hoover and Parrinello-Rahman, respectively. Equilibration was performed for 50 ns and 100 ns for the pure bilayers and peptide containing bilayers, respectively. The production simulations were carried out for up to 200 ns for pure lipid membranes, and 1 μs for the A β_{25-35} containing systems. The last 100 ns and 500 ns, respectively, were used for system analysis. The bilayer thickness was calculated based on the distribution density of phosphorus atoms of the lipid head groups using the in-house tools.

Results

The structural behavior was investigated for model membrane systems based on zwitterionic DMPC with or without the anionic DMPS (denoted as DMPC/PS and DMPC,

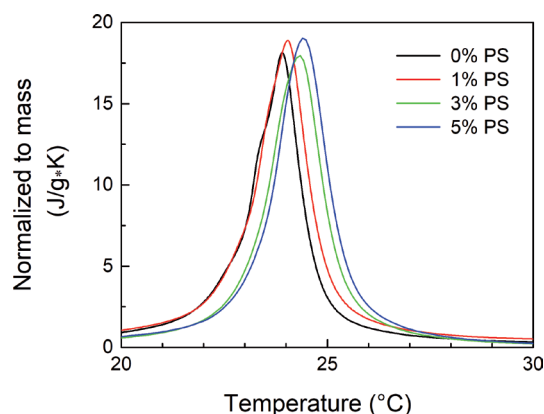


Figure 1. DSC thermograms obtained for the systems of DMPC with various content of anionic lipid DMPS (1, 3 and 5 mol%). The peak positions that depict the main phase transitions of the systems show a negligible dependence on the concentration of DMPS.

respectively). As the membrane thermodynamic phase has been identified previously as a key factor, the main phase transition temperatures of these systems have been determined first. Performed DSC experiments show a small shift in the phase transition temperature to the higher values upon the addition of an increasing amount of anionic lipid into the membrane (Fig. 1). The overall changes are however very small, and can be deemed negligible concerning the further results.

The structural properties of model systems under investigation were analyzed based on the small angle neutron scattering (SANS) experiments. The SANS curves were collected at various temperatures below and above the main phase transitions determined previously for control systems of neat DMPC and DMPC/PS membranes. The scattering curves for systems with DMPS concentrations up to 3 mol% and with or without the addition of A β ₂₅₋₃₅ (denoted as DMPC/A β ₂₅₋₃₅ and DMPC/PS/A β ₂₅₋₃₅) can be found in Figure 2.

The inverse relation between the scattering and direct space allows one to recognize visually the characteristic length-scales based on the features of scattering data profile. According to the simple relation $q = 2\pi/D$, the objects with a characteristic size of 600 Å (e.g., our EULVs) provide in the scattering curve a recognizable feature (e.g., a dip) at $q \sim 0.01 \text{ \AA}^{-1}$. The fingerprint of half the size objects (e.g., our SULVs) appears at $q \sim 0.02 \text{ \AA}^{-1}$. Finally, the imprint of length-scales characteristic to the membrane thickness (i.e., $D \sim 60 \text{ \AA}$) is determined mainly by the region around $q = 0.1 \text{ \AA}^{-1}$. Nevertheless, the advanced analysis of scattering curves is best performed over the entire q -range accessible in the experiment. The extracted parameters are then interconnected according to the complex structural model that is used to approximate the experimental data.

Based on our SANS data, we can evaluate the temperature induced variations in the membrane thickness and overall object size and shape quantitatively when utilizing models. We employ a 3-shell vesicle model and a model of randomly oriented cylindrical shells with circular cross-section that have proved appropriate previously (Ivankov et al. 2021). Briefly, 3-shell vesicle model is a model of spherical object bounded by a single bilayer of lipids and containing aqueous solution inside. The bilayer is divided to 3 layers comprised of lipid headgroups, hydrocarbon chains, and headgroups again, respectively. The second model, used to approximate BLSs, consists of randomly oriented cylindrical shells with circular cross-section and a core-shell structure. The core represents the hydrocarbon chains, and the shell represents the lipid headgroups. Most importantly, the distinctive features of the two models described allow us to unambiguously assign the shape of the object to the scattering data profile, because an inappropriate model provides a poor fit result as opposed to the satisfactory result obtained in the case of fitting the data with the appropriate model.

Considering our previous results (Ivankov et al. 2021), we expect the membranes to reorganize from BLSs to SULVs during the phase transition in the systems with incorporated peptides, while the neat systems should show EULVs undisturbed. Results for DMPC displayed in Figure 2 indeed show all the SANS curves characteristic of the scattering from EULVs, while the changes in results obtained for DMPC/A β ₂₅₋₃₅ displayed in figure corroborate the previously reported effect of A β ₂₅₋₃₅ driven reorganizations between ULVs and BLSs. The changes are clearly seen in SANS data profiles when heating samples above 30°C. A smooth data profile changes by the appearance of a dip in the curves, corresponding to the formation of highly monodisperse ULVs characteristic of smaller sizes than the pores used in extrusion procedure – denoted thus SULVs. The data profile returns back to being smooth when decreasing temperature below 30°C again.

Systems with the DMPS included show similar behavior of the SANS data profiles as those of the neat DMPC systems. Results obtained for DMPC/DMPS systems displayed in Figure 2 confirm all the curves being very similar to each other and corresponding again to typical data profiles for EULVs. Similarly, the SANS curves for the peptide-incorporated DMPC/DMPS membranes suggest the same reorganization of membranes from BLSs to SULVs in a response to the temperature crossing the membrane phase transition, as it was observed in the case of DMPC/A β ₂₅₋₃₅ systems (Fig. 2).

Discussion

The changes of the bilayer thickness obtained from the best-fit results and compared relative to that produced by a neat DMPC bilayer at $T = 20^\circ\text{C}$ are shown in Figure 3A. In agreement with previous results (Kučerka et al. 2011) the thickness is decreasing with the temperature increasing from 20°C up to 45°C, and then it increases as the temperature decreases back to 20°C for all the presented systems. The DMPC/PS systems show a small dependence on the DMPS concentration that causes the membrane thickness increase compared to the pure DMPC systems (Fig. 3A). The bilayer increase is expected due to a less bulky PS headgroup that allows more compact packing of lipids laterally, thus extending in length (Pan et al. 2014).

The additional increase in the bilayer thickness is brought up by the incorporation of A β ₂₅₋₃₅ (temperatures between 35°C and 45°C), and even more dramatic thickness increase is observed for the membranes forming BLSs (temperatures below 35°C) in accordance with the previous results for DMPC/A β ₂₅₋₃₅ systems (Ivankov et al. 2021). We note that the dramatic thickness increase is most likely a direct result of the BLS formation, as the same effect has been documented

previously in the case of common bicelles-forming system even without the addition of a peptide (Yamada 2012).

Figure 3B shows the sizes of the studied objects as obtained from the best-fit results. The heating and cooling across the main phase transition temperature provide again the fully

reversible transformations as observed previously in the case of DMPC/A β_{25-35} and DPPC/A β_{25-35} systems (Ivankov et al. 2021). It is worth noting that the transformations in the current experiment are happening at temperatures by about 6°C higher than the membrane main phase transition tem-

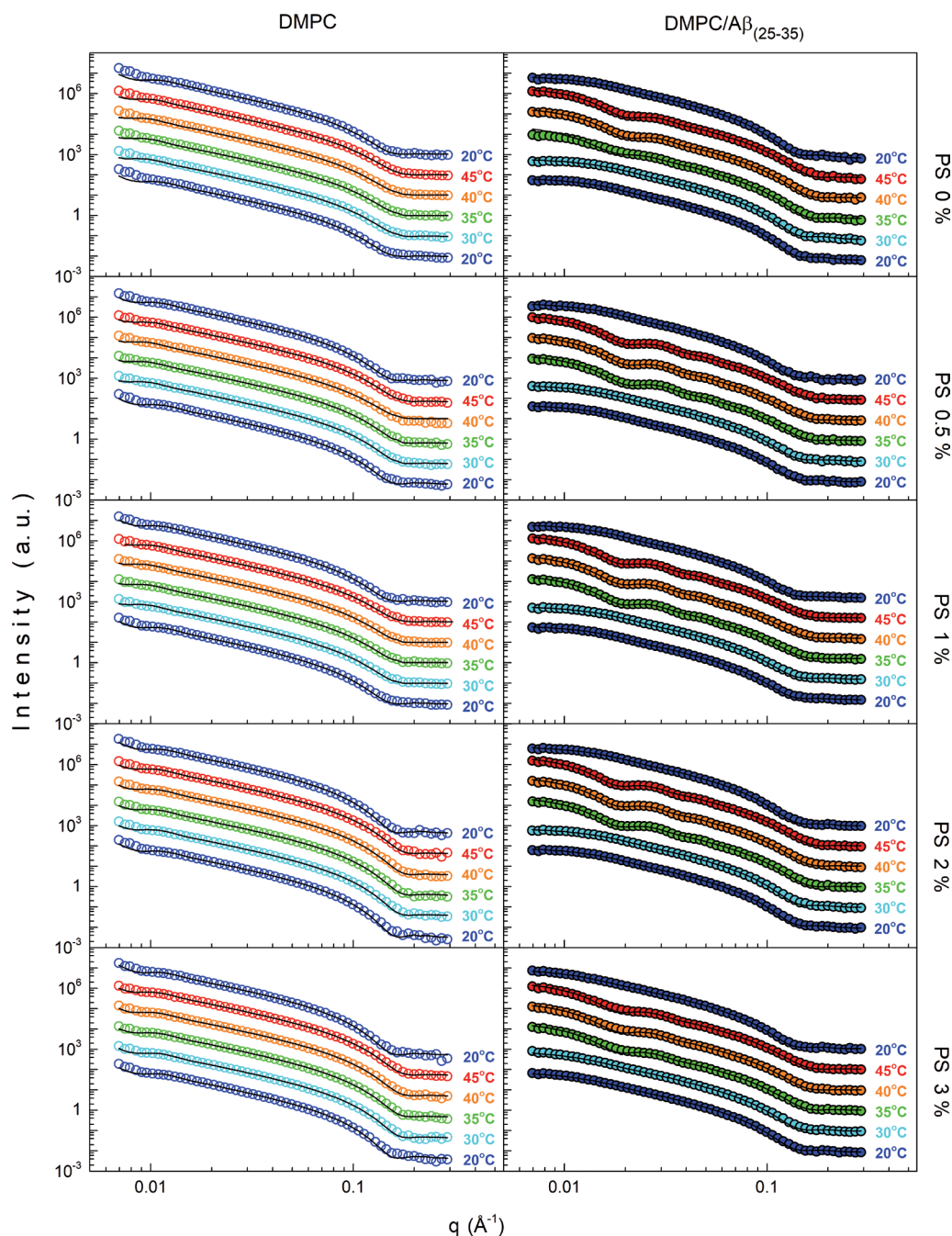


Figure 2. SANS curves for the DMPC, DMPC/A β_{25-35} , DMPC/0.5% PS, DMPC/0.5% PS/A β_{25-35} , DMPC/1% PS, DMPC/1% PS/A β_{25-35} , DMPC/2% PS, DMPC/2% PS/A β_{25-35} , DMPC/3% PS, DMPC/3% PS/A β_{25-35} . Different colors correspond to different measurement temperatures. The data are presented with a y-axis offset for the clarity of presentation. The solid lines correspond to the best fits according to an appropriate model approximation as described in text.

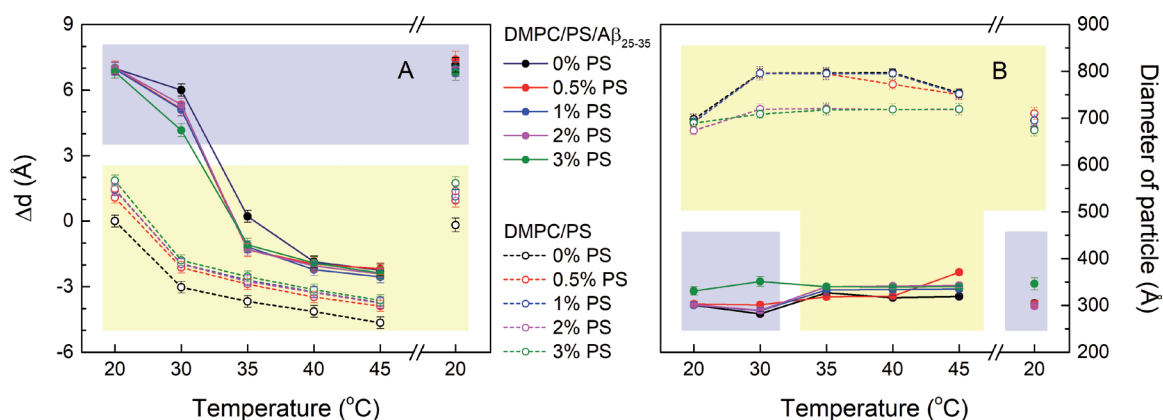


Figure 3. The relative changes to membrane thickness Δd (A) and the diameter of BLSs and ULVs (B) obtained as the best-fit results of SANS curves. The systems of DMPC and DMPC/PS are shown by dashed lines and hollow circles, and those of DMPC/ $A\beta_{25-35}$ and DMPC/PS/ $A\beta_{25-35}$ by solid lines and solid circles. The thickness changes are shown with respect to the neat DMPC bilayer thickness obtained at $T = 20^\circ\text{C}$.

perature. This has been observed previously during the first heating cycles in particular, and most likely advocates the metastable character of the system. Importantly, the observed changes show a similar influence of $A\beta_{25-35}$ whether it is incorporated in the zwitterionic or anionic lipid systems. Both types of the membrane were found to form BLSs below 30°C and reform into SULVs over the range of 30 to 35°C .

The impact of the underlying membrane charge has been reported previously in the case of membrane structure itself or the location of peptide in its interior (Dante et al. 2002; Dies et al. 2014). Our results confirm such observation in part. Perhaps more importantly, however, our data allow us to conclude little impact of the membrane charge

on its destabilization triggered by the peptide during the phase changes. A closer look at the structural parameters of membrane aggregates (Fig. 3) and the form of these aggregates as obtained from SANS data fitting (Fig. 2) reveals a little influence of the anionic lipid on the morphological changes in the systems with incorporated peptides. This in fact may suggest a main driving force of the BLSs-to-ULVs transformation being independent of charge while related rather to the membrane fluidity.

We extend our experimental observations further by evaluating the structural organization of our model systems *via* MD calculations. Firstly, the temperature driven changes to the membrane thickness of various systems are presented in Figure 4. Similarly to the experiment, the membrane thickness shows an increase due to addition of $A\beta_{25-35}$. The influence of the addition of DMPS to the membrane, on the other hand, is not so clearly extracted from MD calculations. In both cases of the neat systems and those with $A\beta_{25-35}$, the difference of the thickness is less than 1 \AA and it does not change systematically with the DMPS concentration. We thus deem the impact of DMPS undifferentiated by MD simulations while concluding their uncertainty within 1 \AA .

In addition to the comparison with experimentally obtained structural results, MD simulations allow us to expand our investigations regarding the dynamics of the studied systems. Namely, we evaluate the effect of charge and $A\beta_{25-35}$ incorporation on the packing and lipid chain order that relates to the dynamics of the lipids (Poger and Mark 2012). Figure 5A documents insignificant changes in the calculated order parameter S_{CD} due to addition of anionic DMPS, though it is somewhat more visible in the gel phase (20°C) when compared to the fluid phase (30°C and 50°C). Intriguingly, this effect increases for the membranes with

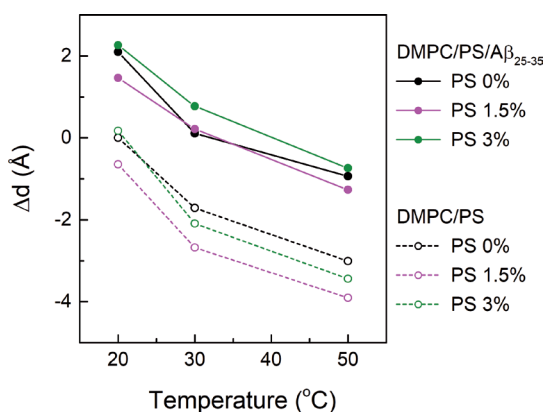


Figure 4. The relative changes to membrane thickness Δd extracted from MD simulations of DMPC/PS systems (hollow circles and dashed lines) and DMPC/PS systems containing $A\beta_{25-35}$ (solid circles and solid lines). The thickness changes are shown with respect to the neat DMPC bilayer thickness obtained at $T = 20^\circ\text{C}$.

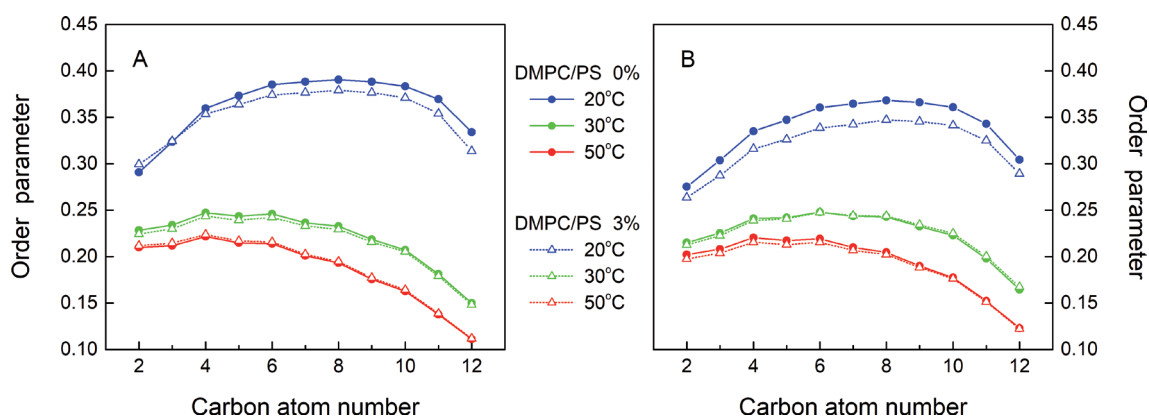


Figure 5. Lipid chain order parameter S_{CD} as a function of hydrocarbon position for model bilayers based on DMPC with or without the addition of 3% DMPS (A), and those with A β_{25-35} incorporated (B). The results were extracted from MD simulations performed at $T = 20^\circ\text{C}, 30^\circ\text{C}, 50^\circ\text{C}$.

incorporated A β_{25-35} (see Fig. 5B), while again mostly in the gel phase (20°C). In the L_α phase (30°C and 50°C), there are practically no changes in the order parameters calculated along the lipid chains of zwitterionic or anionic lipids in the case of systems with or without A β , which is in a good agreement with findings in literature (Labbé et al. 2013). Combining both experimental results and MD calculations we thus conclude a little role of anionic lipid in the A β_{25-35} interactions with the membrane when it is in the fluid phase, while these interactions become more pronounced when the gel phase brings the membrane into more rigid state.

Conclusions

Our SANS experiment performed with the model membranes doped with anionic lipids extends our previous findings of the A β -triggered morphological changes in the zwitterionic lipid systems. Namely, we have documented a reorganization of model membranes from spherical unilamellar vesicles to planar bicelle-like membranes during the membrane phase transitions when amyloid- β peptide A β_{25-35} was present in the membrane. The experimental results show a little influence of the charge on the given reorganization of the system, though we have noticed minor differences in structural parameters such as membrane thickness and size of objects it forms. Combining these results with the results of MD simulations, we suggest the main role in the discussed morphological transformations being played by the membrane crossing the main phase transition temperature. It allows us to propose the changes in rigidity of the membrane being the determining feature in the lipid-peptide interactions leading to the membrane destruction.

Acknowledgments. This work has been supported by the Russian Science Foundation (grant number 19-72-20186). We acknowledge the utilization of IBR-2 facility through its user program and access to the HybriLIT heterogeneous computing platform.

Conflicts of interest. The authors declare no conflicts of interest in regard to this manuscript.

References

- Accardo A, Shalabaeva V, Cotte M, Burghammer M, Krahne R, Riekel C, Dante S (2014): Amyloid β peptide conformational changes in the presence of a lipid membrane system. *Langmuir* **30**, 3191-3198 <https://doi.org/10.1021/la500145r>
- Barrett MA, Alsop RJ, Hauss T, Rheinstadter MC (2015): The position of Abeta22-40 and Abeta1-42 in anionic lipid membranes containing cholesterol. *Membranes (Basel)* **5**, 824-843 <https://doi.org/10.3390/membranes5040824>
- Bokvist M, Lindström F, Watts A, Gröbner G (2004): Two types of Alzheimer's β -amyloid (1-40) peptide membrane interactions: Aggregation preventing transmembrane anchoring versus accelerated surface fibril formation. *J. Mol. Biol.* **335**, 1039-1049 <https://doi.org/10.1016/j.jmb.2003.11.046>
- Breßler I, Kohlbrecher J, Thünemann AF (2015): SASfit: a tool for small-angle scattering data analysis using a library of analytical expressions. *J. Appl. Crystallogr.* **48**, 1587-1598 <https://doi.org/10.1107/S1600576715016544>
- Buchsteiner A, Hauß T, Dencher NA (2012): Influence of amyloid- β peptides with different lengths and amino acid sequences on the lateral diffusion of lipids in model membranes. *Soft Matter*. **8**, 424-429 <https://doi.org/10.1039/C1SM06823G>
- Buchsteiner A, Hauß T, Dante S, Dencher NA (2010): Alzheimer's disease amyloid- β peptide analogue alters the ps-dynamics of phospholipid membranes. *Biochim. Biophys. Acta Biomembr.* **1798**, 1969-1976

- <https://doi.org/10.1016/j.bbmem.2010.06.024>
Dante S, Hauss T, Dencher NA (2002): β -amyloid 25 to 35 is intercalated in anionic and zwitterionic lipid membranes to different extents. *Biophys. J.* **83**, 2610-2616
[https://doi.org/10.1016/S0006-3495\(02\)75271-5](https://doi.org/10.1016/S0006-3495(02)75271-5)
- Dies H, Toppozini L, Rheinstädter MC (2014): The interaction between amyloid- β peptides and anionic lipid membranes containing cholesterol and melatonin. *PLoS One* **9**, e99124
<https://doi.org/10.1371/journal.pone.0099124>
- Hellstrand E, Sparr E, Linse S (2010): Retardation of A β fibril formation by phospholipid vesicles depends on membrane phase behavior. *Biophys. J.* **98**, 2206-2214
<https://doi.org/10.1016/j.bpj.2010.01.063>
- Heo CE, Park CR, Kim HI (2021): Effect of packing density of lipid vesicles on the A β 42 fibril polymorphism. *Chem. Phys. Lipids* **236**, 105073
<https://doi.org/10.1016/j.chemphyslip.2021.105073>
- Ivankov O, Murugova TN, Ermakova EV, Kondela T, Badreeva DR, Hrubovčák P, Soloviov D, Tsarenko A, Rogachev A, Kuklin AI, Kučerka N (2021): Amyloid-beta peptide (25-35) triggers a reorganization of lipid membranes driven by temperature changes. *Sci. Rep.* **11**, 21990
<https://doi.org/10.1038/s41598-021-01347-7>
- Jo S, Kim T, Iyer VG, Im W (2008): CHARMM-GUI: A web-based graphical user interface for CHARMM. *J. Comput. Chem.* **29**, 1859-1865
<https://doi.org/10.1002/jcc.20945>
- Klauda JB, Venable RM, Freites JA, O'Connor JW, Tobias DJ, Mondragon-Ramirez C, Vorobyov I, MacKerell AD, Pastor RW (2010): Update of the CHARMM all-atom additive force field for lipids: Validation on six lipid types. *J. Phys. Chem. B* **114**, 7830-7843
<https://doi.org/10.1021/jp101759q>
- Kubo T, Nishimura S, Kumagai Y, Kaneko I (2002): In vivo conversion of racemized β -amyloid ([D-Ser26]A β 1-40) to truncated and toxic fragments ([D-Ser26]A β 25-35/40) and fragment presence in the brains of Alzheimer's patients. *J. Neurosci. Res.* **70**, 474-483
<https://doi.org/10.1002/jnr.10391>
- Kučerka N, Nieh M-P, Katsaras J (2011): Fluid phase lipid areas and bilayer thicknesses of commonly used phosphatidylcholines as a function of temperature. *Biochim. Biophys. Acta Biomembr.* **1808**, 2761-2771
<https://doi.org/10.1016/j.bbmem.2011.07.022>
- Kuklin AI, Rogachev AV, Soloviov DV, Ivankov OI, Kovalev YS, Utrobin PK, Kutuzov SA, Soloviev AG, Rulev MI, Gordeliy VI (2017): Neutronographic investigations of supramolecular structures on upgraded small-angle spectrometer YuMO. *J. Phys. Conf. Ser.* **848**, 012010
<https://doi.org/10.1088/1742-6596/848/1/012010>
- Labbé J-F, Lefèvre T, Guay-Bégin A-A, Auger M (2013): Structure and membrane interactions of the β -amyloid fragment 25-35 as viewed using spectroscopic approaches. *Phys. Chem. Chem. Phys.* **15**, 7228-7239
<https://doi.org/10.1039/c3cp44623a>
- Orädd G, Lindblom G (2004): NMR studies of lipid lateral diffusion in the DMPC/gramicidin D/water system: Peptide aggregation and obstruction effects. *Biophys. J.* **87**, 980-987
<https://doi.org/10.1529/biophysj.103.038828>
- Pampel A, Kärger J, Michel D (2003): Lateral diffusion of a transmembrane peptide in lipid bilayers studied by pulsed field gradient NMR in combination with magic angle sample spinning. *Chem. Phys. Lett.* **379**, 555-561
<https://doi.org/10.1016/j.cplett.2003.08.093>
- Pan J, Cheng X, Monticelli L, Heberle FA, Kučerka N, Tieleman DP, Katsaras J (2014): The molecular structure of a phosphatidylserine bilayer determined by scattering and molecular dynamics simulations. *Soft Matter.* **10**, 3716-3725
<https://doi.org/10.1039/c4sm00066h>
- Poger D, Mark AE (2012): Lipid bilayers: The effect of force field on ordering and dynamics. *J. Chem. Theory Comput.* **8**, 4807-4817
<https://doi.org/10.1021/ct300675z>
- Selivanova OM, Surin AK, Ryzhykau YL, Glyakina AV, Suvorina MY, Kuklin AI, Rogachevsky VV, Galzitskaya OV (2018): To be fibrils or to be nanofilms? Oligomers are building blocks for fibril and nanofilm formation of fragments of A β peptide. *Langmuir* **34**, 2332-2343
<https://doi.org/10.1021/acs.langmuir.7b03393>
- Soloviev AG, Solovjeva TM, Ivankov OI, Soloviov DV, Rogachev AV, Kuklin AI (2017): SAS program for two-detector system: seamless curve from both detectors. *J. Phys. Conf. Ser.* **848**, 012020
<https://doi.org/10.1088/1742-6596/848/1/012020>
- Sugiura Y, Ikeda K, Nakano M (2015): High membrane curvature enhances binding, conformational changes, and fibrillation of amyloid- β on lipid bilayer surfaces. *Langmuir* **31**, 11549-11557
<https://doi.org/10.1021/acs.langmuir.5b03332>
- Tang J, Alsop RJ, Backholm M, Dies H, Shi A-C, Rheinstädter MC (2016): Amyloid- β 25-35 peptides aggregate into cross- β sheets in unsaturated anionic lipid membranes at high peptide concentrations. *Soft Matter.* **12**, 3165-3176
<https://doi.org/10.1039/C5SM02619A>
- Van Der Spoel D, Lindahl E, Hess B, Groenhof G, Mark AE, Berendsen HJC (2005): GROMACS: Fast, flexible, and free. *J. Comput. Chem.* **26**, 1701-1718
<https://doi.org/10.1002/jcc.20291>
- Wildburger NC, Esparza TJ, LeDuc RD, Fellers RT, Thomas PM, Cairns NJ, Kelleher NL, Bateman RJ, Brody DL (2017): Diversity of amyloid-beta proteoforms in the Alzheimer's disease brain. *Sci. Rep.* **7**, 9520
<https://doi.org/10.1038/s41598-017-10422-x>
- Yamada NL (2012): Kinetic process of formation and reconstruction of small unilamellar vesicles consisting of long- and short-chain lipids. *Langmuir* **28**, 17381-17388
<https://doi.org/10.1021/la302684z>
- Yoda M, Miura T, Takeuchi H (2008): Non-electrostatic binding and self-association of amyloid β -peptide on the surface of tightly packed phosphatidylcholine membranes. *Biochem. Biophys. Res. Commun.* **376**, 56-59
<https://doi.org/10.1016/j.bbrc.2008.08.093>

Received: July 11, 2022

Final version accepted: October 17, 2022